

# Spatial Organization and Stoichiometry of N-Terminal Domain-Mediated Glycosyltransferase Complexes in Golgi Membranes Determined by FRET Microscopy

Mariana L. Ferrari · Guillermo A. Gomez ·  
Hugo J. F. Maccioni

Received: 31 October 2011/Revised: 13 January 2012/Accepted: 20 February 2012/Published online: 3 March 2012  
© Springer Science+Business Media, LLC 2012

**Abstract** The functional link between glycolipid glycosyltransferases (GT) relies on the ability of these proteins to form organized molecular complexes. The organization, stoichiometry and composition of these complexes may impact their sorting properties, sub-Golgi localization, and may determine relative efficiency of GT in different glycolipid biosynthetic pathways. In this work, by using Förster resonance energy transfer microscopy in live CHO-K1 cells, we investigated homo- and hetero-complex formation by different GT as well as their spatial organization and molecular stoichiometry on Golgi membranes. We find that GalNAcT and GalT2 Ntd are able to form hetero-complexes in a 1:2 molar ratio at the *trans*-Golgi network and that GalT2 but not GalNAcT forms homo-complexes. Also, GalNAcT/GalT2 complexes exhibit a stable behavior reflected by its clustered lateral organization. These results reveals that particular topological organization of GTs may have functional implications in determining the composition of glycolipids in cellular membranes.

Special Issue: In Honor of Bob Ledeen

This work is dedicated to Bob Ledeen, a pioneer in the study of the biochemistry and neurochemistry of glycolipids, great friend and enthusiastic and clever investigator.

M. L. Ferrari · G. A. Gomez · H. J. F. Maccioni (✉)  
Departamento de Química Biológica, Facultad de Ciencias Químicas, Centro de Investigaciones en Química Biológica de Córdoba, CIQUIBIC (UNC-CONICET), Universidad Nacional de Córdoba, Ciudad Universitaria, 5000 Córdoba, Argentina  
e-mail: maccioni@mail.fcq.unc.edu.ar

**Present Address:**

G. A. Gomez  
Division of Molecular Cell Biology, Institute for Molecular Bioscience, The University of Queensland, St. Lucia, Brisbane, QLD 4072, Australia

**Keywords** Golgi complex · Glycosyltransferase complexes · Live cell FRET microscopy · Glycolipids

## Introduction

Glycolipids are synthesized in the Golgi apparatus membranes by integral membrane glycolipid glycosyltransferases (GT). The majority of these enzymes are Golgi resident, type II transmembrane proteins, with an N-terminal domain (Ntd), comprising a short cytoplasmic tail (CT), a transmembrane region (TMR) and a short stem region, and a luminal C-terminal, catalytic domain. Transcriptional and post transcriptional regulatory mechanisms acting on GT influence the wide repertoire of glycolipids produced by cells [1]. Ganglioside biosynthesis is coupled and compartmentalized in the Golgi apparatus [2]. Glycosylation of LacCer, GM3 and GD3 to form simple ganglioside species occurs in proximal and distal Golgi subcompartments. On the other hand, synthesis of more complex gangliosides is displaced towards the most distal compartments of the Golgi apparatus and the *trans*-Golgi network (TGN) [3]. Evidence has been provided about Golgi enzyme associations in many glycosylation pathways, as well as on the different domains involved in the associations [4, 5]. It has been described that the N-terminal domain of GTs are necessary and sufficient to confer Golgi localization to GTs [6, 7] and are involved in covalent and non-covalent associations in some glycosyltransferase complexes, in addition to other reported associations mediated by the catalytic domain [5, 8]. However, in vivo evidence about the participation of Ntds in the formation of enzyme homo- or hetero-complexes, on their spatial organization in the Golgi membranes and about their stoichiometry in these associations is lacking. In this work we address these issues using Förster resonance energy transfer

(FRET) microscopy focusing on Golgi membranes of live CHO-K1 cells. In particular, we investigate the ability of the Ntd domains of GalT2, GalNAcT, SialT2 and GalT1 to form complex associations by fusing them to appropriate spectral variants of the GFP. Results indicate that GalT2 Ntd are able to form homo-complexes in the Golgi membranes and that the GalNAcT/GalT2 hetero-complex shows a clustered distribution in the Golgi membranes with a stoichiometry of the association of 1:2.

## Experimental Procedures

### Plasmids

The plasmids pECFP-N1 and pEYFP-N1 were from Clontech (CA, USA). The plasmid of the fusion protein CFP-YFP was a gift of J. L. Daniotti (CIQUIBIC), and was constructed with the enhanced versions of the fluorescent proteins (Clontech, CA, USA). The plasmids pSCFP-C1 and pSYFP-C1 with monomeric versions of cyan and yellow fluorescent proteins, respectively, were a gift of T. Gadella (Swammerdam Institute for Life Sciences, University of Amsterdam, The Netherlands) [9] and their N1 versions were performed by A. Trenchi (CIQUIBIC, Argentina). The plasmids encoding the Ntd of GalNAcT, GalT2, Sial-T2, Sial-T1 or Gal-T1 fused to ECFP or EYFP were previously described [6, 7]. Glycosyltransferases Ntd attached to monomeric SCFP and SYFP were performed replacing the enhanced fluorescent proteins by the monomeric versions using *BamHI* and *NotI* restriction sites.

### Cell Culture and Transfection

CHO-K1 cells (ATCC, Manassas, VA, USA) were maintained at 37°C, 5% CO<sub>2</sub> in Dulbecco's modified Eagle's medium (DMEM) supplemented with 10% fetal bovine serum (FBS) and antibiotics (ATB, 100 µg/ml penicillin and 100 µg/ml streptomycin). Cells were transfected with 0.8–1.0 µg/35 mm dish of the indicated plasmid using cationic liposomes (Lipofectamine, Invitrogen, CA, USA). At 24 h after transfection, the cells were plated onto 8-well glass chamber slides (LabTek, NUNC, Naperville, IL, USA). After culture the cells for 36 h, the culture medium was replaced by DMEM, 10% FBS with no phenol red and the cells were used for live cell imaging.

### Live Cell Imaging for FRET Analyses

Confocal images for FRET analysis were collected using an Olympus Fluoview™ FV1000 confocal microscope (Olympus Latin America, Miami, FL) equipped with a multi-line Argon laser (458, 488 and 514 nm) and two Helium Neon

lasers (543 and 633 nm). CFP fluorescence was detected by using laser excitation at 458 nm, a 458/514 nm excitation dichroic mirror and a 470–500 nm bandpass emission filter. YFP fluorescence was detected by using laser excitation at 514 nm, a 458/514 nm excitation dichroic mirror and a 530–570 nm bandpass emission filter. Live cell experiments were performed at 37°C (Tritech DigiTherm temperature controller, CA, USA). Images were sequentially acquired in line mode, Kalman 2, collecting the signal by photon counting. Images were taken using a 100X UPlanSApo oil immersion/1.4 NA objective (Olympus, Japan), 2–3 × digital zoom, 320 × 320 image resolution, Kalman line 2, and adjusting the pinhole to obtain an optical slice of 0.8–1 µm. The acquisition conditions were optimized to minimize bleaching and scanning time but maximizing signal-to-noise ratio of the different images.

### Sensitized Emission FRET Quantitative Analysis and Image Analysis

Postacquisition *cell-by-cell* image analysis and quantification were performed with ImageJ 1.42I (NIH, <http://rsbweb.nih.gov/ij/>). We used the algorithm previously described by Elangovan et al. [10] to remove donor cross-talk (CT<sub>D</sub>) and acceptor bleedthrough (BT<sub>A</sub>) contaminants in the FRET signal, using seven images: two single-labeled donor reference images (D<sub>ex</sub>/D<sub>em</sub> and D<sub>ex</sub>/A<sub>em</sub>); two single-label acceptor reference images (D<sub>ex</sub>/A<sub>em</sub> and A<sub>ex</sub>/A<sub>em</sub>); and three double-labeled images (A<sub>ex</sub>/A<sub>em</sub>, D<sub>ex</sub>/D<sub>em</sub> and D<sub>ex</sub>/A<sub>em</sub>). The D<sub>ex</sub>/D<sub>em</sub> shows the quenched donor (qD) fluorescence and corresponds to the donor channel (D), whereas the A<sub>ex</sub>/A<sub>em</sub> indicates the acceptor fluorescence and corresponds to the acceptor channel (A). The D<sub>ex</sub>/A<sub>em</sub> corresponds to the uncorrected FRET (uFRET) image, which is then processed by Elangovan algorithm to generate the precision-FRET (PFRET) image, showing the corrected energy transfer levels:

$$\text{PFRET} = \text{uFRET} - \text{qD} \cdot \text{CT}_D - \text{A} \cdot \text{BT}_A \quad (1)$$

Pseudocolored PFRET images were generated with ImageJ 1.42I (NIH, <http://rsbweb.nih.gov/ij/>); red is the GalNAcT/GalT2-normalized maximum PFRET value, and black corresponds to the minimum value, 0.

The energy transfer efficiency

$$E = 1 - \frac{\text{qD}}{\text{uD}} \quad (2)$$

is expressed as a percentage of the fluorescence of donor in the absence of FRET, or unquenched donor uD. This last parameter was calculated as

$$\text{uD} = \text{qD} + \text{PFRET} \quad (3)$$

as an approximation of Eq. B.19 in [10]. ImageJ and SigmaPlot 10.0 were used to calculate this parameter. We

first generated in ImageJ two binary masks for the D and A channels where pixels with donor intensity and acceptor intensity values higher and lower than the corresponding background signal were set to a value equal to 1 and 0, respectively [11]. After obtaining these two masks, we multiplied them in a pixel by pixel basis to obtain a colocalization mask, which represents the position of those pixels where both qD and A signals were significant. Significant pixels from qD, A and PFRET images were obtained by multiplying these images with the corresponding colocalization mask. Then, mean values for these parameters were quantified in each cell in a region covering the entire Golgi area. We restricted the data analysis to identical areas in the three uD, A and PFRET images. Mean **E** values were calculated for each ROIs according to

$$E = 1 - \frac{qD}{qD + PFRET} \quad (4)$$

For **E** normalization, first GalNAcT/GalT2 **E** value was determined in *n* ROIs; GalNAcT/GalT2 mean **E** was calculated with all the ROIs, and then, **E** for each ROI of GalNAcT/GalT2 as well as the other GTs co-expression was divided by the previously calculated GalNAcT/GalT2 mean **E**.

To obtain the data to perform membrane distribution analysis, small ROIs corresponding to Golgi structures larger than 8 pixels were defined using the ImageJ Analyze Particles plugin. Usually each Golgi from a single cell give from 10 to 30 of such small structures containing both Donor and Acceptor molecules. The mean values of qD, A and PFRET of these small regions of interest were then used to calculate the unquenched donor (uD), acceptor (A), mean FRET efficiency (**E**) and uD/A ratio. To establish the confidence interval (CI) for random distribution in **E** vs uD/A plots, using the negative control data GalNAcT/GalNAcT for each experiment we randomly reassigned each **E** value of a given ROI to a different ROI, performing this for all measured ROIs. The randomization step was performed 5,000 times using MatLab and for each ROI mean **E** and its standard deviation were calculated. These data were plotted as Mean **E** ± 95% CI of uD/A to describe the boundaries of the randomized variables.

To test if there was correlation between **E** and A values for a given experiment, we perform linear regression analysis of the variables in order to capture correlation between them.

### Stoichiometry Analysis

In order to calculate the uD and A stoichiometry by sensitized emission FRET, we firstly determined a correction factor, *R*, that take into account the CFP and YFP fluorescence variations due to fluorophores quantum yield (*Q*),

detection efficiency ( $\Gamma$ ), molar extinction coefficients ( $\epsilon$ ) and number of fluorescent molecules (*n*). The *R* factor was determined in each experiment by using the CFP-YFP linked construct, where the stoichiometry is 1:1, i.e., the molar fraction of D or A is 0.5. With the mean uD and A values, we calculated the A fluorescent fraction, as

$$X_{FA} = \frac{A}{A + uD} \quad (5)$$

As the total A fluorescence in a given volume is the fluorescence of one molecule multiplied by the total number of molecules at low concentrations, we can state that the A fluorescence fraction is

$$X_{FA} = \frac{1}{1 + \frac{n_D \cdot F_{uD}}{n_A \cdot F_{IA}}}, \quad (6)$$

where *n* is the number of donor or acceptor molecules, and  $F_{uD}$  or  $F_{IA}$  is the mean fluorescence per molecule which is related to the quantum yield and extinction coefficient of a given fluorophore and detection conditions. For the linked construct,  $n_D = n_A$ . The mean stoichiometry correction factor  $R = \frac{F_{uD}}{F_{IA}}$  was determined experimentally as

$$R = \left[ \frac{1}{X_{FA}} \right] - 1 \quad (7)$$

Using this correction factor, then the acceptor molar fraction  $X_A = \frac{n_A}{n_A + n_D}$  for each Golgi apparatus of each cell was calculated as

$$X_A = \frac{R \cdot A}{R \cdot A + uD} \quad (8)$$

to determine GalT2 and GalNAcT stoichiometry.

## Results

### Characterization of Glycolipid Glycosyltransferases Heterocomplexes by FRET in Live CHO-K1 Cells

FRET is a phenomenon that reports molecular proximity between pairs of fluorophores on a length scale of 1–10 nm [12–14]. In combination with fluorescence confocal microscopy, FRET measurement is a versatile technique that allows determination of the lateral organization (clustered or random) of molecules in their natural environment in live cells. Using this technique we aimed to investigate the ability of different GT to form homo- and hetero-complexes and to determine their spatial organization and molecular stoichiometry in Golgi membranes. For this, we co-expressed in CHO-K1 cells different pairs of glycosyltransferase Ntd fused to cyan fluorescent protein (CFP) as FRET donor or yellow fluorescent protein (YFP) as FRET

acceptor. Under these conditions spectral contamination occurs due to overlapping donor and acceptor emission spectra (donor cross-talk), and also due to acceptor excitation at the donor excitation wavelength (acceptor bleed-through). To process the images with a correction algorithm [10], confocal microscopy images were collected for donor, acceptor and uncorrected FRET (uFRET) channels from cells expressing only donor or acceptor molecules or co-expressing both donor and acceptor molecules (Fig. 1a–d). Pixel-by-pixel corrected FRET (Precision-FRET, PFRET) images were obtained (Fig. 1a–d, right), with the energy transfer levels represented in pseudo-colors [10]. Co-expressed soluble CFP and YFP served as FRET negative control, because of their mean intermolecular distance in the cytoplasm of cells is considerable larger than the Förster distance for CFP and YFP [15].

GalNAcT and GalT2 Ntd were in the Golgi apparatus close enough to undergo FRET between the fused donor and acceptor [6] (Fig. 1a). Regarding the other glycosyltransferases pairs assayed, although co-expressed SialT2/GalNAcT, SialT2/GalT2 or GalNAcT/GalT1 co-localized in the Golgi apparatus, they displayed lower energy transfer levels (Fig. 1b–d), close to the values given by the co-expressed soluble CFP and YFP (negative control) (Fig. 1e). Figure 1f is the plot of the mean FRET efficiency in Golgi ( $E$ ) normalized by the mean GalNAcT/GalT2  $E$ .

#### GalT2 but not GalNAcT form Detectable Homo-Complexes

It was also considered of interest to analyze whether glycolipid glycosyltransferases Ntd were able to interact to form homo-complexes. To this end, live cells co-expressing the Ntd of the glycosyltransferases under study fused at the C-terminus to both CFP and YFP (Fig. 2a, b), were examined for FRET. GalNAcT/GalT2 and GalNAcT/GalT1 pairs were used as positive and negative controls, respectively. PFRET positive signal was detected in particular zones of the Golgi apparatus of cells co-expressing GalT2 Ntd (Fig. 2a), and at levels comparable to those of GalNAcT/GalT2 (Fig. 1a). We confirmed that GalT2 Ntd are indeed involved in homo-complex formation using monomeric variants of CFP and YFP and hence discarding that GalT2 oligomerization was induced by self aggregation of enhanced fluorescent proteins (not shown). In contrast, GalNAcTCFP/GalNAcTYFP Ntd pairs display PFRET signal just at background levels (Fig. 2b). The quantitative analysis showed that mean  $E$  in Golgi membranes (Fig. 2c) was slightly higher for GalT2/GalT2 Ntd pairs than for GalNAcT/GalT2 Ntd pairs. Also,  $E$  was significantly higher ( $p < 0.05$ ) in GalT2/GalT2 Ntd pairs than in GalNAcT/GalT1 Ntd pairs, the latter two enzymes known to concentrate in different sub-compartments of the

Golgi apparatus [7, 16]. Mean  $E$  for GalNAcT/GalNAcT Ntd pairs was as for the negative control and significantly lower ( $p < 0.05$ ) than GalT2/GalT2 Ntd pairs. These data indicate that contrary to GalT2 Ntd, GalNAcT Ntd do not form detectable homo-complexes in Golgi apparatus membranes.

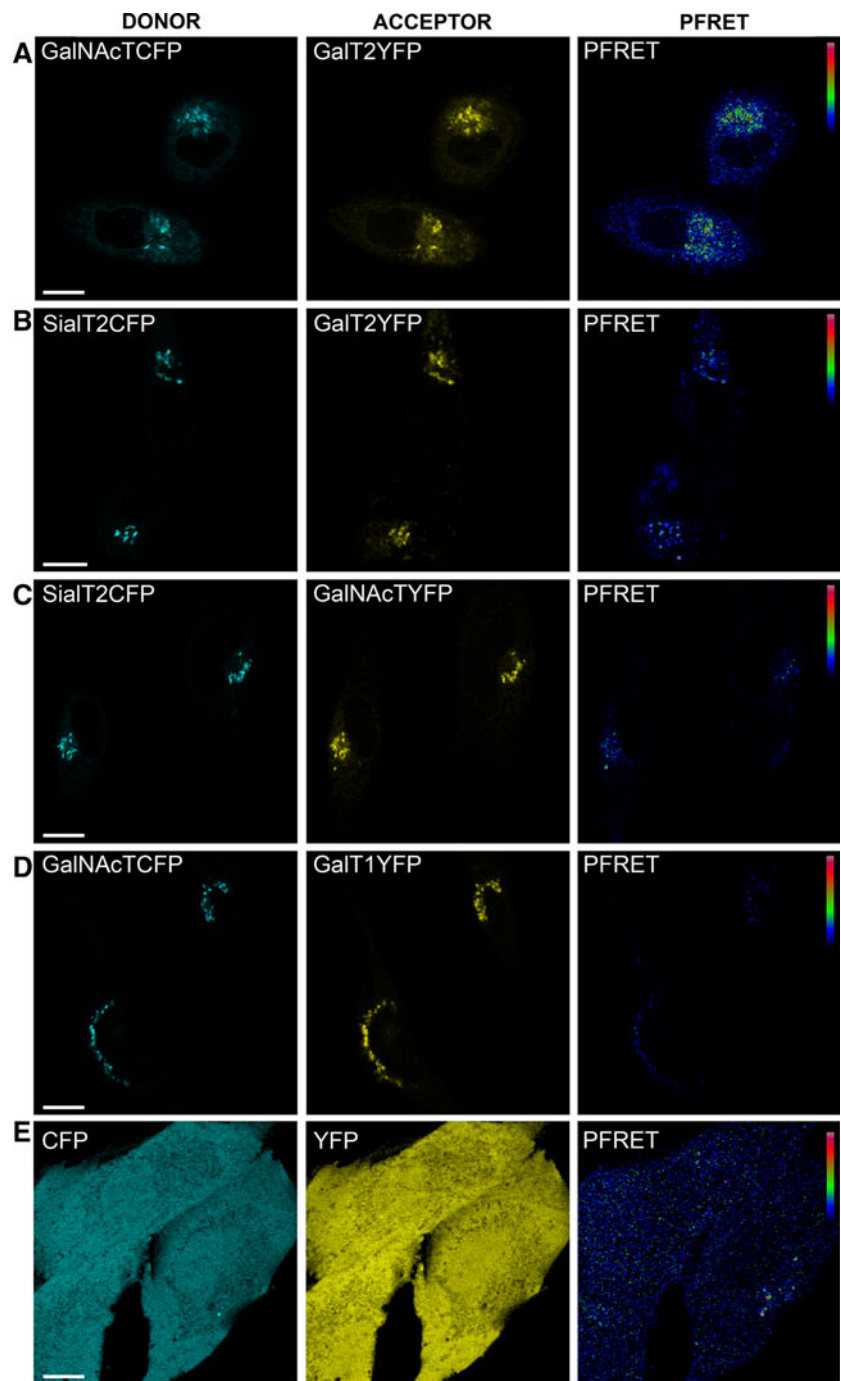
#### Molecular Clustering of Glycosyltransferases

As FRET is a measure of molecular proximity, it is a consequence of the lateral distribution of molecules in membranes. Mathematical models have been developed describing random or clustered distribution of molecules in cellular membranes. These models are based in FRET efficiency analysis as a function of both acceptor surface density and of the ratio between unquenched donor (uD), which is the donor in the absence of FRET, and acceptor (A) (uD/A ratio) (Fig. 3). Two experimental parameters are indicative of molecular clustering: independence of  $E$  from acceptor levels (Fig. 3a) and negative dependence of  $E$  on uD/A ratio (Fig. 3b) [17, 18].

To determine whether GalNAcT/GalT2 complexes are distributed in clusters in Golgi membranes, their Ntd tagged with CFP or YFP were co-expressed, and the dependence of  $E$  from acceptor (GalT2YFP) levels and uD/A ratio (GalNAcTCFP/GalT2YFP) was evaluated. The analyzed ROIs corresponded only to Golgi structures where both enzymes co-localized. Results indicate that, in the range of A levels analyzed,  $E$  is poorly correlated with A levels in Golgi membranes, and do not decrease toward zero with decreasing A levels (Fig. 3a, *GalNAcT/GalT2*). The lack of correlation between  $E$  values and acceptor intensity levels was confirmed by regression analysis ( $p = 0.2649$ ), which shows no significant difference compared to random distributed variables (Fig. 3a, *GalNAcT/GalT2*). Regarding  $E$  dependence with uD/A ratio, the obtained values show a strongly negative dependence with uD/A ratio increment (Fig. 3b, *GalNAcT/GalT2*), suggesting that GalNAcT/GalT2 complexes occur clustered in the Golgi membranes. In this case randomized  $E$  values for each uD/A ratio for a negative control GalNAcT/GalNAcT (see below) produced a graph significantly different (Fig. 3b, *GalNAcT/GalT2*, dotted lines), thus statistically supporting the finding of a clustered organization. Taken together, these results indicate that FRET between GalNAcT and GalT2 is occurring due to a clustered organization rather than to molecular crowding and random collisions in the Golgi membranes.

To further validate our conclusion about the clustered organization of the GalNAcT/GalT2 pair, we performed the same analysis for the GalNAcT/GalNAcT pair. This is a pair that does not form stable complexes and so we can assume that the only chance of undergoing FRET is due to

**Fig. 1** FRET microscopy revealed GalNAcT/GalT2 Ntd heterocomplex formation in Golgi membranes of live CHO-K1 cells. **a–e** Donor (cyan), acceptor (yellow) and PFRET (pseudocolor) images of representative cells co-expressing different glycosyltransferase Ntd pairs. FRET levels are represented by the pseudocolor scale bar in PFRET images, where blue and red correspond to background and high FRET values, respectively. GalNAcT/GalT2 Ntd exhibited PFRET in some Golgi apparatus regions (**a**). SialT2/GalT2 (**b**), SialT2/GalNAcT (**c**) and GalNAcT/GalT1 (**d**) Ntd, although colocalized in Golgi regions, did not exhibit significant PFRET levels. Co-expression of soluble CFP and YFP (**e**) was used as FRET negative control. *Bar*, 10  $\mu\text{m}$ . **f** Mean *E* values in Golgi were normalized by the mean GalNAcT/GalT2 *E* value. All the pairs assayed exhibited significantly lower *E* values than GalNAcT/GalT2 pair ( $*p < 0.05$ , Student's *t* test over three independent experiments.  $N > 75$  cells in each case) (Color figure online)



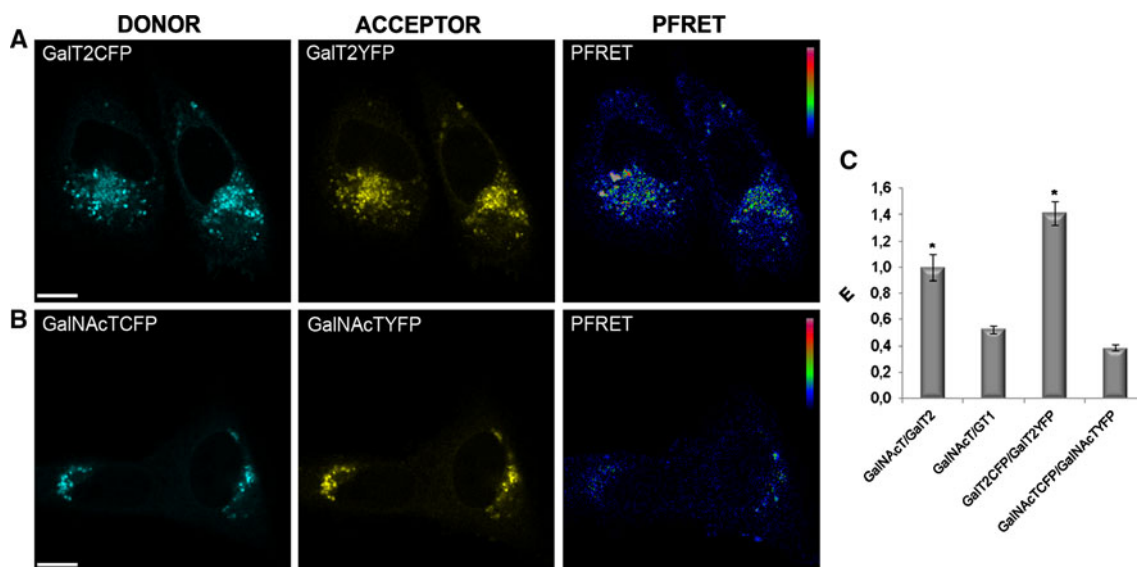


**Fig. 2** FRET microscopy revealed GalT2 homo-complexes formation in Golgi membranes of live CHO-K1 cells. **a–b** Donor (cyan), acceptor (yellow) and PFRET (pseudocolor) images of representative cells co-expressing GalT2 or GalNAcT Ntd pairs. FRET levels are represented by the pseudocolor scale bar as in Fig. 1. Cells co-expressing Ntd of both GalT2CFP and GalT2YFP (**a**) exhibited significant PFRET levels in Golgi regions. On the other hand, the co-expression of GalNAcTCFP/GalNAcTYFP displayed PFRET signal just at background levels (**b**). Bar, 10  $\mu\text{m}$ . (**c**), For each GT

co-expression, mean **E** value was determined in the Golgi, normalized by the positive control GalNAcT/GalT2 mean **E** value and plotted. **E** for GalT2CFP/GalT2YFP co-expression was in the order of GalNAcT/GalT2 hetero-complex and was significantly higher than the negative control GalNAcT/GalT1 co-expression ( $*p < 0.05$ , Student's *t* test over three independent experiments.  $N > 75$  cells in each case). On the other hand, **E** for GalNAcTCFP/GalNAcTYFP co-expression was below **E** for GalNAcT/GalT1 co-expression (Color figure online)

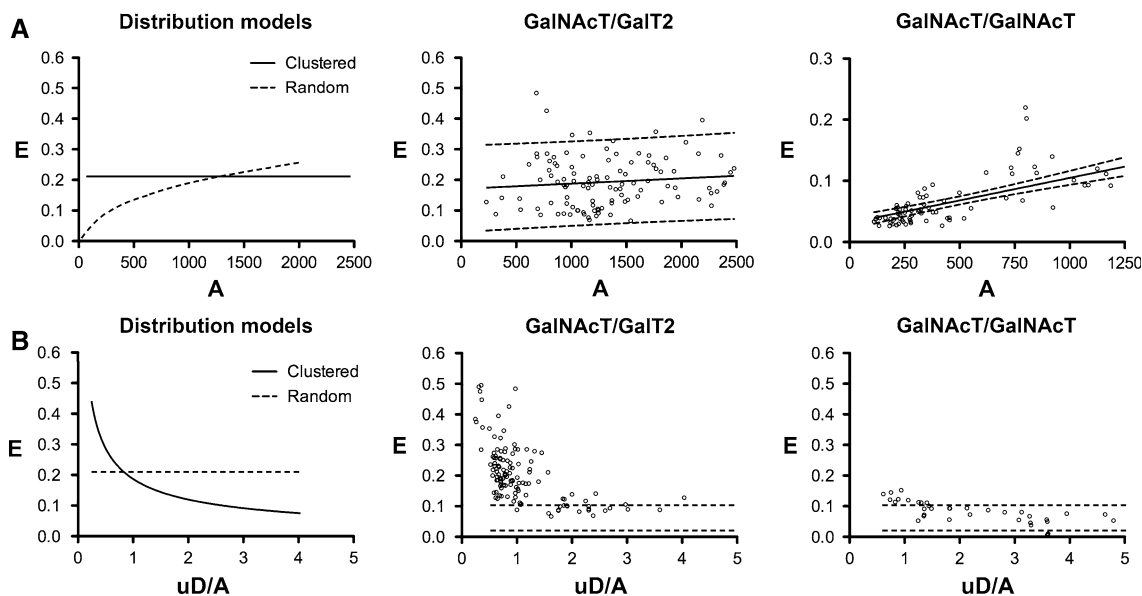


**Fig. 3** Glycosyltransferase complex distribution in Golgi membranes. **a**, Left, Predicted **E** values as a function of acceptor levels in membranes for clustered (continuous line) and random (dashed line) distribution models. Actual **E** value distributions as a function of acceptor levels obtained from cells co-expressing GalNAcT/GalT2 (center) or GalNAcT/GalNAcT (right) are given. A linear regression of the data was performed (continuous lines) and confidence intervals (95%) are shown (dashed lines). For GalT2/GalNAcT a no significant

( $p = 0.2649$ ) and for GalNAcT/GalNAcT a significant ( $p < 0.0001$ ) correlation was found. **b** Left, Predicted **E** values as a function of uD/A ratio for clustered (continuous line) and random (dashed line) distribution models. Actual **E** distribution values as a function of uD/A ratio for GalT2/GalNAcT (center) and for GalNAcT/GalNAcT co-expression (right) are given. **E** values of each ROI for GalNAcT/GalNAcT pair were randomized across different ROIs. Dotted lines show the confidence interval (95%) of the simulated data

molecular crowding and random collisions (Fig. 3a and b, *GalNacT/GalNacT*). By analyzing the dependence of **E** versus **A** for this pair we found a significant positive correlation between these two parameters, also validated by linear regression analysis ( $p < 0.0001$ ) (Fig. 3a, *GalNacT/GalNacT*). On the other hand, no correlation was observed for **E** and **uD/A** values (Fig. 3b, *GalNacT/GalNacT*). Moreover, the observed distribution of **E** versus **uD/A** values was between the confidence intervals that represents random behavior (Fig. 3b, *GalNacT/GalNacT*, dotted lines). Overall, the positive correlation of **E** versus **A** and the lack of correlation between **E** versus **uD/A** for the *GalNacT/GalNacT* pair, validate our approach to characterize the spatial organization of GTs in Golgi membranes.

### Stoichiometry of GalNacT/GalT2 Hetero-Complex

It was considered of interest to know the stoichiometry of GalNacT and GalT2 in the enzyme complex they participate of. For this, we determined **E** by confocal microscopy in living cells to investigate the molar ratio of donor and acceptor molecules that form Ntd mediated GT complexes. As we measure intermolecular FRET by sensitized emission, the bright of fluorescent donor and acceptor molecules may not directly correlate with their molecular abundance, since other factors as quantum yield, extinction coefficients, and detection efficiency affect fluorescence intensity. To correct for these factors, in addition to donor cross-talk and acceptor bleed-through corrections, it was necessary to normalize donor and acceptor fluorescence intensity in the samples before translating them to enzyme abundance in the complex.

To this end, a stoichiometry correction factor *R*, which is the ratio between donor fluorescence per molecule and acceptor fluorescence per molecule, was obtained by expressing a linked tandem construct of donor and acceptor (CFP-YFP), in which FRET is expected to occur and in which the molar ratio is 1:1. Mean FRET efficiency (**E**) by cell was determined for the linked CFP-YFP pair, the *R* correction factor was calculated and applied in every experiment to determine the molar ratio of the participating proteins from fluorescence microscopy data (see “[Experimental Procedures](#)”).

We first collected confocal images of GalNacTCFP and GalT2YFP co-expressing cells and determined pixel-by-pixel PFRET values (Fig. 1a), verifying that energy transfer was occurring in some Golgi areas. An appropriate threshold was applied to this PFRET image to isolate regions in cells with only PFRET significant values. **uD**, **A** and *R* correction factor values were used to calculate the mean molar ratio of acceptor ( $X_A = \text{GalT2YFP}$ ) per cell (Eq. 8, see “[Experimental Procedures](#)”). The histogram of

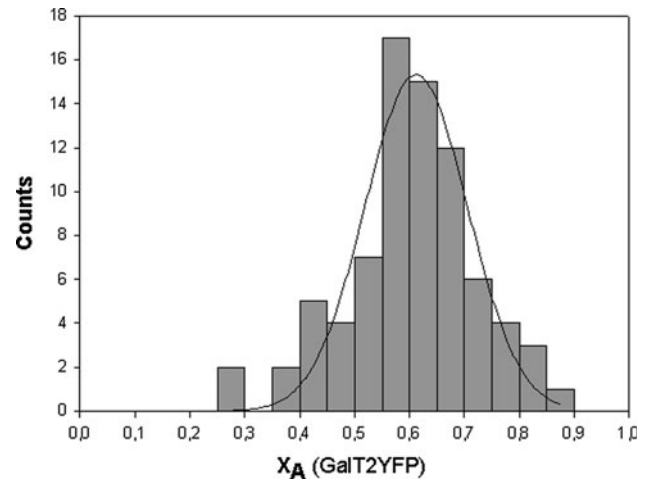


**Fig. 4** Frequency histogram of acceptor molar fraction ( $X_A = \text{GalT2YFP}$ ) in GalNacT/GalT2 hetero-complex. The stoichiometry correcting factor, *R*, was determined expressing in cells the tandem construct CFP-YFP, as indicated under Experimental procedures. **uD**, **A** and *R* were used to calculate the mean molar ratio of acceptor ( $X_A = \text{GalT2YFP}$ ) in each ROI, corresponding to Golgi apparatus. Maximum frequency occurs in ROIs with a GalT2YFP molar fraction of 0.62, indicating the highest probability of FRET occurrence at a molar ratio GalNacT:GalT2 about 1:2. Counts in the histogram are the number of ROIs with the indicated acceptor molar ratio. Results are representative of two independent experiments

$X_A$  (GalT2YFP) frequency distribution is shown in Fig. 4. The maximum frequency occurs at GalT2YFP molar fraction of 0.62, equivalent to a GalNacTCFP molar fraction of 0.38, indicating that the highest probability of FRET occurrence between GalNacT and GalT2 Ntd in Golgi membranes is at a molar ratio about 1:2.

### Discussion

Previous studies from this laboratory showed that glycolipid glycosyltransferases form at least two multienzyme complexes with participation of their Ntd in CHO-K1 cells, one formed by GalT1, SialT1 and SialT2 [7], mainly of proximal Golgi localization, and the other formed by GalT2 and GalNacT, localized to the *trans*-Golgi and TGN [6].

In a follow up of these studies, herein we investigated in the Golgi apparatus of live CHO-K1 cells: (a) if GalT2 and GalNacT Ntd, in addition to form an hetero-complex, also form homo-complexes; (b) if GalT2 and GalNacT Ntd interactions are due to molecular clustering or to molecular crowding in the Golgi membranes; and (c) the GalNacT:GalT2 Ntd stoichiometry in the hetero-complex. For this we applied a FRET microscopy technique that allows assessment of interactions among molecules in regions of interest of live cells [10, 19]. FRET in live cells circumvent

potential risks of artifacts of other technologies used to study molecular interactions. A common technique is co-immunoprecipitation starting from cell lysates, in which random mixing of components due to abrogation of sub-cellular compartments may give rise to interactions between molecules that in the cell are set apart and hence without possibilities of mutual interactions. Furthermore, the use of different antibodies against the proteins under study in co-immunoprecipitations makes the determination of binding affinities and stoichiometry of partners in the complex very difficult.

FRET is a nonradiative phenomenon in which part of the energy absorbed by a donor fluorophore is transferred to an acceptor molecule. It occurs when donor and acceptor fluorophores have a proximity of 1–10 nm, favorable dipole–dipole interaction and sufficiently spectral overlap [12–14]. Given these conditions, FRET results in donor fluorescence quenching and acceptor fluorescence increment. As this effect depends on the sixth power inverse of the distance between donor and acceptor [20], it is extremely sensitive to determine molecular proximity.

#### Formation of GTs Hetero- and Homo-Complexes

Results obtained indicate that GalNAcT and GalT2 Ntd were in the Golgi apparatus close enough to undergo FRET between the fused donor and acceptor fluorophores. SialT2/GalNAcT, SialT2/GalT2 or GalNAcT/GalT1, although also co-localized in the Golgi apparatus, displayed no significant FRET values. Data also indicate that GalT2 Ntd, but not GalNAcT Ntd, form homo-complexes in Golgi apparatus membranes. The simplest interpretation for results in (a) is that hetero-complex formation occurs between the Ntd of enzymes that colocalize in a given Golgi subcompartment. GalNAcT is a TGN concentrated enzyme, while GalT2 concentrate in the distal Golgi although extend its presence to the TGN by complexing GalNAcT, as it was previously demonstrated by colocalization with Golgi/TGN markers, and Brefeldin A and nocodazole treatment of cells [7, 21]. The more proximal Golgi localization of SialT2 and GalT1 would preclude molecular proximity enough to undergo FRET with GalNAcT. The formation of homo-complexes of GalT2 but not of GalNAcT Ntd is intriguing, indicating that not only the co-localization is determinant in complex formation, but other functional mechanisms are involved. One is tempting to hypothesize that GalT2 homo-complexes may constitute a reserve pool of GalT2 to accompany developmental fluctuations of GalNAcT, known to act as a key regulatory enzyme at the GM3 branching point that directs the flow of intermediates towards the “a” or “b” pathway gangliosides [2, 22, 23]. It is also possible that GT homo-complex as well as hetero-complex formation act as sorting

or as Golgi retention mechanisms, as it was previously proposed for other protein complexes (reviewed in [24]). In this regard, it is interesting to note that wild type CHO-K1 cells do not express GalNAcT. However, GalT2 is able to exit the ER and to reach and concentrate in the Golgi apparatus of these cells, suggesting that homo-complex formation may be relevant for subcellular distribution and sorting of GTs. The use of more sophisticated techniques, such as three-color spectral FRET [25] may be useful to study the *in vivo* distribution profiles of GalT2, as monomer, homo-complex and hetero-complex, when expressed alone or in combination with GalNAcT.

#### GalT2 and GalNAcT Ntd Complexes Occurs in Clusters on Golgi Membranes

We considered important to distinguish between two situations in which FRET between partners could occur: molecular crowding and molecular clustering. This is particularly critical when exogenous expression of the fusion proteins is being carried out, since overexpression may overcome natural relationships between membrane bound proteins, leading to artifactual results. Evaluation of FRET efficiency dependence on GalT2YFP acceptor levels and on donor GalNAcTCFP/acceptor GalT2YFP ratio indicate that FRET between GalNAcT and GalT2 is allowed by a clustered organization rather than by molecular crowding in the Golgi membranes. In addition, the lack of detection of GalNAcT homo-complexes, when GalNAcT Ntds fused to D and A are co-expressed in Golgi membranes, indicates that enzyme overexpressions not necessarily implicates molecular crowding and FRET occurrence.

#### GalNAcT/GalT2 Ntd Stoichiometry

*Application* to FRET values of an additional correction factor that normalizes the bright of fluorescent donor and acceptor molecules to their molecular abundance, allowed determining that the highest probability of FRET occurrence between GalNAcT and GalT2 Ntd in Golgi membranes is at a molar ratio about 1:2. Since the specific catalytic activity of the enzymes in their natural membrane environment is not known, we cannot extrapolate mass ratio data to enzyme activity data. However, since the  $K_m$  for the respective acceptors and  $V_{max}$  are in the same order for both GalNAcT (117  $\mu\text{M}$ ; 6  $\text{nmol mg h}^{-1}$ ) [26] and GalT2 (22  $\mu\text{M}$ ; 16  $\text{nmol mg h}^{-1}$ ) [27], and assuming similar fractional saturation of each enzyme with the corresponding sugar nucleotide donors [2], it is possible to hypothesize that the observed molar ratio would assure a displacement of the sequence of conversion of GM3 towards formation of GM1. In fact, over-expression of



transfected GalNAcT in CHO-K1 cells, which lack GalNAcT but express endogenous GalT2, results in major consumption of GM3 and accumulation of GM1 and GD1a with only traces of GM3 and few GM2 remaining [21].

Examination of the amino acid sequence of the Ntd of both GalNAcT (aa 1–27) and GalT2 (aa 1–52) shows presence of two cysteine residues in the transmembrane of GalNAcT (cysteines 9 and 17) but absence of cysteine residues in the sequence of GalT2. This precludes the possibility that the homo- and hetero- complexes we are describing here are formed by disulfide bridges, as occurs in the full length GalNAcT [28]. Rather, it seems that hydrophobic forces acting between the transmembrane regions may drive the interactions.

As mentioned above, we focused on the interactions that may operate at the level of the Ntds of GT. An enzyme complex formed by full-length SialT2 and GalNAcT in F-11A cells, a substrain of neuroblastoma F-11 cells [29], has been reported, and recently homo- and hetero-complexes of glycoprotein glycosyltransferases have been described using bimolecular fluorescence complementation (BiFC) [30] and FRET flow cytometric quantification [8]. In the latter study, although the catalytic domains are mainly involved in enzyme interactions, Ntd are responsible for complex formation in some cases. Further studies will be necessary to know the relative contributions of different associative ways that may operate in the full length glycolipid glycosyltransferases.

**Acknowledgments** This work was supported in part by Grants from Agencia Nacional de Promoción Científica y Tecnológica (PICT-2006-01239), Universidad Nacional de Córdoba, y MinCyT Córdoba. We thank the technical assistance of G. Schachner and S. Deza with cell cultures and of C. Mas and M. C. Sampedro with confocal microscopy. M.L.F. and G.A.G. were recipients of CONICET Fellowships and H.J.F.M. is Career Investigator of CONICET (Argentina).

## References

1. Yu RK, Bieberich E, Xia T, Zeng G (2004) Regulation of ganglioside biosynthesis in the nervous system. *J Lipid Res* 45(5):783–793
2. Maxzud MK, Daniotti JL, Maccioni HJ (1995) Functional coupling of glycosyl transfer steps for synthesis of gangliosides in Golgi membranes from neural retina cells. *J Biol Chem* 270(34):20207–20214
3. Maccioni HJ (2007) Glycosylation of glycolipids in the Golgi complex. *J Neurochem* 103(Suppl 1):81–90
4. de Graffenried CL, Bertozzi CR (2004) The roles of enzyme localisation and complex formation in glycan assembly within the Golgi apparatus. *Curr Opin Cell Biol* 16(4):356–363
5. Young WW Jr (2004) Organization of Golgi glycosyltransferases in membranes: complexity via complexes. *J Membr Biol* 198(1):1–13
6. Giraudo CG, Daniotti JL, Maccioni HJ (2001) Physical and functional association of glycolipid N-acetyl-galactosaminyl and galactosyl transferases in the Golgi apparatus. *Proc Natl Acad Sci USA* 98(4):1625–1630
7. Giraudo CG, Maccioni HJ (2003) Ganglioside glycosyltransferases organize in distinct multienzyme complexes in CHO-K1 cells. *J Biol Chem* 278(41):40262–40271
8. Hassinen A, Pujol FM, Kokkonen N, Pieters C, Kihlstrom M, Korhonen K, Kellokumpu S (2011) Functional organization of Golgi N- and O-glycosylation pathways involves pH-dependent complex formation that is impaired in cancer cells. *J Biol Chem* 286(44):38329–38340
9. Kremers GJ, Goedhart J, van Munster EB, Gadella TW Jr (2006) Cyan and yellow super fluorescent proteins with improved brightness, protein folding, and FRET Forster radius. *Biochemistry* 45(21):6570–6580
10. Elangovan M, Wallrabe H, Chen Y, Day RN, Barroso M, Periasamy A (2003) Characterization of one- and two-photon excitation fluorescence resonance energy transfer microscopy. *Methods* 29(1):58–73
11. Trenchi A, Gomez GA, Daniotti JL (2009) Dual acylation is required for trafficking of growth-associated protein-43 (GAP-43) to endosomal recycling compartment via an Arf6-associated endocytic vesicular pathway. *Biochem J* 421(3):357–369
12. Jares-Erijman EA, Jovin TM (2003) FRET imaging. *Nat Biotechnol* 21(11):1387–1395
13. Lippincott-Schwartz J, Snapp E, Kenworthy A (2001) Studying protein dynamics in living cells. *Nat Rev Mol Cell Biol* 2(6):444–456
14. Wallrabe H, Periasamy A (2005) Imaging protein molecules using FRET and FLIM microscopy. *Curr Opin Biotechnol* 16(1):19–27
15. Hoppe A, Christensen K, Swanson JA (2002) Fluorescence resonance energy transfer-based stoichiometry in living cells. *Biophys J* 83(6):3652–3664
16. Uliana AS, Giraudo CG, Maccioni HJ (2006) Cytoplasmic tails of SialT2 and GalNAcT impose their respective proximal and distal Golgi localization. *Traffic* 7(5):604–612
17. Kenworthy AK, Edidin M (1998) Distribution of a glycosylphosphatidylinositol-anchored protein at the apical surface of MDCK cells examined at a resolution of <100 Å using imaging fluorescence resonance energy transfer. *J Cell Biol* 142(1):69–84
18. Wallrabe H, Elangovan M, Burchard A, Periasamy A, Barroso M (2003) Confocal FRET microscopy to measure clustering of ligand-receptor complexes in endocytic membranes. *Biophys J* 85(1):559–571
19. Gordon GW, Berry G, Liang XH, Levine B, Herman B (1998) Quantitative fluorescence resonance energy transfer measurements using fluorescence microscopy. *Biophys J* 74(5):2702–2713
20. Förster T (1948) Zwischenmolekulare Energiewanderung und Fluoreszenz. *Ann Physik* 6(2):55–75
21. Giraudo CG, Rosales Fritz VM, Maccioni HJ (1999) GA2/GM2/GD2 synthase localizes to the trans-golgi network of CHO-K1 cells. *Biochem J* 342(Pt 3):633–640
22. Panzetta P, Maccioni HJ, Caputto R (1980) Synthesis of retinal gangliosides during chick embryonic development. *J Neurochem* 35(1):100–108
23. Yu RK, Macala LJ, Taki T, Weinfield HM, Yu FS (1988) Developmental changes in ganglioside composition and synthesis in embryonic rat brain. *J Neurochem* 50(6):1825–1829
24. Maccioni HJ, Quiroga R, Ferrari ML (2011) Cellular and molecular biology of glycosphingolipid glycosylation. *J Neurochem* 117(4):589–602
25. Galperin E, Verkhusha VV, Sorkin A (2004) Three-chromophore FRET microscopy to analyze multiprotein interactions in living cells. *Nat Methods* 1(3):209–217
26. Pohlentz G, Klein D, Schwarzmann G, Schmitz D, Sandhoff K (1988) Both GA2, GM2, and GD2 synthases and GM1b, GD1a,

- and GT1b synthases are single enzymes in Golgi vesicles from rat liver. *Proc Natl Acad Sci USA* 85(19):7044–7048
27. Martina JA, Daniotti JL, Maccioni HJ (2000) GM1 synthase depends on N-glycosylation for enzyme activity and trafficking to the Golgi complex. *Neurochem Res* 25(5):725–731
28. Li J, Yen TY, Allende ML, Joshi RK, Cai J, Pierce WM, Jaskiewicz E, Darling DS, Macher BA, Young WW Jr (2000) Disulfide bonds of GM2 synthase homodimers. Antiparallel orientation of the catalytic domains. *J Biol Chem* 275(52):41476–41486
29. Bieberich E, MacKinnon S, Silva J, Li DD, Tencomnao T, Irwin L, Kapitonov D, Yu RK (2002) Regulation of ganglioside biosynthesis by enzyme complex formation of glycosyltransferases. *Biochemistry* 41(38):11479–11487
30. Hassinen A, Rivinoja A, Kauppila A, Kellokumpu S (2010) Golgi N-glycosyltransferases form both homo- and heterodimeric enzyme complexes in live cells. *J Biol Chem* 285(23):17771–17777